

Subfield Scheduling for Throughput Maximization in Electron-Beam Photomask Fabrication

Sergey Babin[†], Andrew B. Kahng[‡], Ion I. Măndoiu[‡], and Swamy Muddu[‡]

[†] Soft Services, P.O. Box 2083, Castro Valley, CA 94546

[‡] ECE and CSE Departments, University of California San Diego, La Jolla, USA 92093
sbabin@softsrv.com, {abk,smuddu}@ucsd.edu, mandoiu@cs.ucsd.edu

ABSTRACT

Resist heating is one of the largest contributors to critical dimension (CD) distortion in electron beam photomask fabrication. Previous methods for reducing CD variation caused by resist heating include lower beam currents, increased delays between electron flashes, and writing in multiple passes. However, all these methods lower mask writing throughput. This leads to increased mask writing cost, which is increasingly becoming a major limiting factor to semiconductor industry productivity.

In this work, we investigate a new degree of freedom for mitigating CD distortion caused by resist heating. By optimizing the sequence in which subfields are being written, it is possible to reduce CD variability caused by resist heating, without significantly increasing the mask writing time.

1. INTRODUCTION

High voltage (50kV) electron beams are needed to improve spatial resolution in mask fabrication using variable-shaped beam (VSB) writers. However, high voltage beams lead to a higher amount of heat being deposited in a smaller area of exposure, and this results in significant critical dimension (CD) distortion.^{1, 2, 4, 5} Maximizing writer throughput under the ever more stringent constraints on CD distortion imposed by design rules for deep-submicron technology nodes requires exploiting all degrees of freedom available in the mask fabrication process. Recent works^{7, 8} have explored the optimization of such parameters as beam current density, flash size, and number of passes. In this paper we propose a complementary approach to throughput maximization, based on scheduling of subfields. By avoiding successive writing of subfields that are close to each other, our approach ensures that resist temperature is maintained below a given threshold, thus limiting CD distortion. Although our subfield scheduling slightly increases beam travel time compared to the standard sequential subfield order, the lower resist temperature enables the use of a higher beam current density, which leads to smaller dwell time. Depending on the particular parameters of the writer, the approach can reduce the total writing time and hence increase throughput while keeping the CD distortion within the desired bounds.

The rest of the paper is organized as follows. In Section 2 we study the computational complexity of the mask writing schedule problem using a simplified formulation based on the notion of blocked set. In Section 3 we present a subfield scheduling scheme based on a class of well-spaced labelings recently introduced by Lagarias.⁹ Finally, in Section 4 we present results of simulation experiments carried out using the commercially available TEMPTATION tool³ and comparing Lagarias subfield scheduling with sequential, random, and spiral subfield schedules.

2. COMPUTATIONAL COMPLEXITY OF THE MASK WRITING SCHEDULE PROBLEM

In this section we formulate the problem of finding an optimum mask writing schedule based on the notion of blocked set. We show that even in this simplified model the problem is NP-hard¹⁰ and hence unlikely to admit efficient exact algorithms.

When a region is being written on the mask, the absorbed energy raises the temperature of neighboring regions. To avoid excessive CD distortion, the following writing step should not occur in a neighboring region that exceeds a certain threshold temperature. We call such a region *blocked for writing*. In the following we

assume that the set of blocked regions and the blocking duration depend on the region itself (shape, area, etc.), but not on the history of events preceding the moment when the region is being written. We also assume that the time to reposition the beam from one region to another is negligible compared to writing times. With these assumptions we obtain the following formulation:

Mask Writing Schedule Problem (MWSP)

Given: A set of n non-overlapping regions R_1, R_2, \dots, R_n in the plane, and, for each region R_i , *writing time* w_i , *blocked set* $B_i \subseteq \{R_1, \dots, R_n\}$, and *blocking duration* d_i .

Find: writing start times $t_i \geq 0$, $i = 1, \dots, n$, for each region such that

1. Two regions are not being written at the same time, i.e., for every $i \neq j$, if $t_i \leq t_j$ then $t_i + w_i \leq t_j$;
2. No region is being written while blocked, i.e., if $R_i \in B_j$ then either $t_j + d_j \leq t_i$ or $t_j > t_i$;
3. The completion time, $\max_i(t_i + w_i)$, is minimized.

THEOREM 2.1. *MWSP is NP-hard, even when restricted to instances with $w_i \equiv d_i \equiv 1$.*

Proof. The proof is by reduction from the directed Hamiltonian path problem, which is known to be NP-hard.¹⁰ For a given directed graph $G = (V, E)$, construct an instance of MWSP in which the regions R_i correspond to the vertices of G , $w_i \equiv d_i \equiv 1$, and B_i consists of all vertices R_j with $(R_i, R_j) \notin E$. It is easy to verify that G has a Hamiltonian path if and only if the MWSP instance admits a writing schedule with no idle time (i.e., completion time equal to n). \square

Remark. MWSP can be approximated within a factor of $1 + \rho$, where

$$\rho = \max_i \frac{d_i}{w_i} \tag{1}$$

by writing the regions in arbitrary order, with an idle time of d_i after writing region R_i for each $i = 1, \dots, n$. The idle times ensure schedule feasibility (whenever writing resumes there is no blocked region). This schedule has a completion time of

$$\sum_{i=1}^n (w_i + d_i) \leq \sum_{i=1}^n (w_i + \rho w_i) = (1 + \rho) \sum_{i=1}^n w_i \tag{2}$$

and $\sum_{i=1}^n w_i$ is trivially a lower-bound on the optimum completion time.

3. SUBFIELD SCHEDULING

Fracture scheduling could result in large increases in writing time due to limitations imposed on the settling time by VSB writer hardware. Scheduling of subfields incurs a smaller overhead in beam travel time. Therefore, in this paper we concentrate on using subfield scheduling to prevent excessive CD distortion due to resist heating.

Let $G(M_1, M_2) = \{(i, j) : 0 \leq i \leq M_1 - 1, 0 \leq j \leq M_2 - 1\}$ be the $M_1 \times M_2$ rectangular grid defined by subfields to be scheduled. Assuming that subfield writing time is constant, we can identify any subfield schedule to a labeling of $G(M_1, M_2)$ with integers from 1 to $M_1 M_2$. Our objective is to find a labeling in which the minimum distance between subfields with consecutive labels is as large as possible. Lagarias⁹ gives a *well-spaced labeling scheme* which addresses this problem when distances are measured under the Manhattan metric, i.e., when the distance between grid locations (i, j) and (i', j') is given by

$$\| (i, j) - (i', j') \| = |i - i'| + |j - j'| \tag{3}$$

An *admissible labeling* of $G(M_1, M_2)$ is a bijection $\phi : [1, M_1 M_2] \rightarrow G(M_1, M_2)$. The 2-spacing $s_2(\phi)$ of a labeling is

$$s_2(\phi) = \min\{\| \phi(m) - \phi(m + 1) \| : 1 \leq m \leq M_1 M_2 - 1\} \tag{4}$$

The circular 2-spacing $s_2^*(\phi)$ is the minimum Manhattan distance between consecutive points in G_{M_1, M_2} , viewing G_{M_1, M_2} as a torus, i.e.,

$$s_2^*(\phi) = \min\{\|\phi(m) - \phi(m+1)\|_T : 1 \leq m \leq M_1 M_2 - 1\} \quad (5)$$

where $\|\cdot\|_T$ is the torus Manhattan metric defined by

$$\|(i, j) - (i', j')\|_T := |(i - i') \bmod M_1| + |(j - j') \bmod M_2| \quad (6)$$

(here $r \bmod M$ denotes the least absolute value residue modulo M). The circular 2-spacing is always greater than the 2-spacing of a labeling.

In the following, we give the Lagarias well-spaced labelings for even and odd number combinations of M_1 and M_2 . These labelings guarantee that the minimum Manhattan distance between subfields with consecutive labels are at most one less than the maximum possible.⁹

Case 1: M_1 and M_2 are both odd.

Set L = least common multiple (l.c.m.) of M_1 and M_2 , G = greatest common divisor (g.c.d.) of M_1 and M_2 . If $m = iL + j$ with $0 \leq i < G$ and $0 \leq j < L$, then

$$\phi(m) = \left(i + j \left(\frac{M_1 - 1}{2} \right) \bmod M_1, j \left(\frac{M_2 + 1}{2} \right) \bmod M_2 \right) \quad (7)$$

Case 2: One of M_1 and M_2 is even and the other is odd.

$$\phi(m) = \left(i + j \frac{M_1}{2} \bmod M_1, j \left(\frac{M_2 - 1}{2} \right) \bmod M_2 \right) \quad (8)$$

Case 3: M_1 and M_2 are both even.

Define

$$\begin{aligned} L^* &= \frac{1}{2} \times \text{l.c.m.}(M_1, M_2) \text{ if } \frac{M_1 M_2}{4} \text{ is odd,} \\ L^* &= \text{l.c.m.}(M_1, M_2) \text{ if } \frac{M_1 M_2}{4} \text{ is even.} \end{aligned} \quad (9)$$

Set $G^* = \text{g.c.d.}(M_1, M_2)$ so that $M_1 M_2 = H^* G^* H^*$, with

$$\begin{aligned} H^* &= 2 \text{ if } \frac{M_1 M_2}{4} \text{ is odd,} \\ H^* &= 1 \text{ if } \frac{M_1 M_2}{4} \text{ is even.} \end{aligned} \quad (10)$$

If

$$m = lG^*L^* + iL^* + j \quad (11)$$

with

$$0 \leq j \leq L^* - 1; 0 \leq i \leq G^* - 1; 0 \leq l \leq H^* - 1, \quad (12)$$

then

$$\phi(m) = \left(l + j \left(\frac{M_1 - 1}{2} \right) \bmod M_1, i + j \left(\frac{M_2 - 2}{2} \right) \bmod M_2 \right) \quad (13)$$

4. SIMULATION SETUP AND PARAMETERS

In this section, we describe the experimental setup for thermal simulations of different subfield writing schedules. The commercial TEMPTATION software³ was used for simulating the thermal evolution of resist on mask during e-beam exposure. We simulated four scheduling strategies:

1. Sequential writing schedule (conventionally used by VSB writers). In this schedule, writing starts at a corner of the major field and proceeds in a sequential serpentine fashion.
2. Lagarias writing schedule. In this schedule, writing is performed according to the order specified by the analytical formulas given in Section 3. The Lagarias order for 16×16 subfields is given in Figure 1.
3. Spiral writing schedule. In this schedule, writing starts at the center of the major field and proceeds outward in a clockwise fashion.
4. Random writing schedule. The random schedule order for 16×16 subfields is given in Figure 2.

We simulated a major field of size $1.024\text{mm} \times 1.024\text{mm}$, divided into 16×16 subfields of size $64\mu\text{m} \times 64\mu\text{m}$ each. For each subfield we simulated a chessboard fracture pattern exposed in sequential-serpent order as shown in Figure 3. For a complete set of parameters used in the TEMPTATION simulations see Tables 1–4.

For each subfield scheduling, the simulation was performed in two phases. In the first simulation phase, each of the 256 subfields was exposed to four coarse flashes that delivered to the subfield the same dose as the detailed chessboard fracture flashes. Furthermore, the four doses were spaced such that subfield writing time was identical to that required by detailed chessboard fracture flashes. This coarse simulation captures the effect of subfield scheduling on the *average* subfield temperature before writing. As a result of first phase simulations we identified for each subfield ordering the subfield with the largest average temperature before writing, which we call “critical” subfield. Detailed fracture flashing was then simulated for each of the four critical subfields corresponding to each ordering.

4.1. Results and Conclusions

Figure 4 shows the temperature before writing for each of the 16×16 subfields under the four considered writing schedules. The Lagarias and random schedules have a lower average subfield temperature compared to the sequential and spiral schedules. The maximum subfield temperature is lower for the Lagarias schedule than for the random one.

Figure 5 shows the temperature before writing for the fractures in the critical subfields corresponding to the four simulated schedules. The results show that the worst fracture temperature before writing for the Lagarias order is reduced to 90.78°C compared to 105.10°C for sequential, 110.70°C for spiral, and 94.77°C for random order. The lower resist temperature enables the use of a higher beam current density. Depending on the particular parameters of the writer, this can reduce total writing time and hence increase throughput while keeping CD distortion within acceptable limits. Ongoing work explores improved scheduling that takes into account beam travel time with simultaneous optimization of beam current density.

REFERENCES

1. N. Kuwahara, H. Nakagawa, M. Kurihara, N. Hayashi, H. Sano, E. Murata, T. Takikawa and S. Noguchi, “Preliminary Evaluation of Proximity and Resist Heating Effects Observed in High Acceleration Voltage E-Beam Writing for 180-nm-and-beyond Rule Reticle Fabrication”, *SPIE Symposium on Photomask and X-Ray Mask Technology VI*, SPIE Vol. 3784, 1999, pp. 115-125.
2. C. A. Mack, “Electron Beam Lithography Simulation for Mask Making, Part VI: Comparison of 10 and 50kV GHOST Proximity Effect Correction”, *Photomask and Next-Generation Lithography Mask Technology VIII*, SPIE Vol. 4409, 2001, pp. 194-203.
3. Sergey Babin, Igor Yu. Kuzmin, “Experimental Verification of the TEMPTATION (temperature simulation) software tool”, *J. Vac. Sci. Technol B* 16(6), 1998, pp. 3241-3247.

Dimensions of main deflection field	$1.024mm \times 1.024mm$
Dimensions of sub deflection field	$64\mu m \times 64\mu m$
Max. Dimension of fracture	$2\mu m \times 2\mu m$
Plate type	Glass
Thickness	$30\mu m$
Density	$2.2g/cm^3$
Thermal Conductivity	0.014
Specific heat	$0.75J/g-K$

Table 1. Mask parameters

Accelerating voltage	50kV
Current Density	$40A/cm^2$
Resist sensitivity	$5\mu C/cm^2$
Maximum shot size	$2\mu m \times 2\mu m$
No. of Subfields in the mask	256
No. of fractures in the subfield	1024
No. of fractures exposed in subfield	512
Exposure time	125ns
Adjacent pattern shot settling time	100ns
Duration of write of single subfield	0.1152ms
Total duration of write (for all subfields)	30ms

Table 2. VSB writer parameters

Resist	ZEP7000
Max. resist thickness	$0.5\mu m$
Density of the resist	$1.1g/cm^3$
Thermal conductivity of the resist	0.0019
Specific heat	$0.980J/g-K$

Table 3. Resist parameters

Substrate	Chrome
Thickness of substrate	$0.08\mu m$
Density of substrate	$7.19g/cm^3$
Thermal Conductivity	0.629
Specific heat	$0.465J/g-K$

Table 4. Substrate parameters

1	17	33	49	65	81	97	113	129	145	161	177	193	209	225	241
248	8	24	40	56	72	88	104	120	136	152	168	184	200	216	232
239	255	15	31	47	63	79	95	111	127	143	159	175	191	207	223
214	230	246	6	22	38	54	70	86	102	118	134	150	166	182	198
205	221	237	253	13	29	45	61	77	93	109	125	141	157	173	189
180	196	212	228	244	4	20	36	52	68	84	100	116	132	148	164
171	187	203	219	235	251	11	27	43	59	75	91	107	123	139	155
146	162	178	194	210	226	242	2	18	34	50	66	82	98	114	130
137	153	169	185	201	217	233	249	9	25	41	57	73	89	105	121
128	144	160	176	192	208	224	240	256	16	32	48	64	80	96	112
103	119	135	151	167	183	199	215	231	247	7	23	39	55	71	87
94	110	126	142	158	174	190	206	222	238	254	14	30	46	62	78
69	85	101	117	133	149	165	181	197	213	229	245	5	21	37	53
60	76	92	108	124	140	156	172	188	204	220	236	252	12	28	44
35	51	67	83	99	115	131	147	163	179	195	211	227	243	3	19
26	42	58	74	90	106	122	138	154	170	186	202	218	234	250	10

Figure 1. Subfield writing sequence for 16×16 Lagarias scheduling

137	131	44	171	130	35	256	124	127	83	149	12	126	195	242	138
14	244	246	170	132	231	77	214	104	207	107	40	163	26	84	229
5	10	70	36	199	56	112	224	220	230	3	205	174	31	45	247
48	18	219	129	59	216	19	147	33	227	122	52	64	102	254	218
118	71	11	200	49	148	140	68	32	146	46	206	198	213	97	164
186	187	156	73	179	6	136	17	42	160	240	1	234	67	177	61
99	90	23	226	53	94	155	217	141	9	135	4	192	75	108	211
43	39	72	204	248	7	212	91	100	54	62	183	167	63	145	223
115	29	66	20	173	188	125	117	197	222	110	25	34	92	235	41
139	89	233	243	252	255	28	185	251	151	55	27	215	22	182	237
194	121	158	103	86	180	95	58	47	16	13	101	81	57	178	60
193	133	79	88	245	98	175	37	253	24	69	74	114	161	80	93
176	172	51	78	105	157	196	113	241	96	191	109	225	144	128	111
166	152	228	15	116	208	154	169	21	168	250	238	232	201	203	153
209	120	30	236	76	239	106	65	50	82	162	123	249	2	134	221
159	8	85	142	143	181	119	202	87	150	165	189	184	38	210	190

Figure 2. Subfield writing sequence for 16×16 random schedule

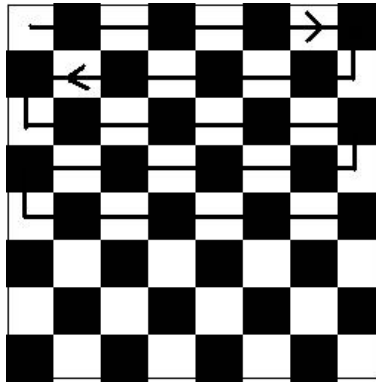


Figure 3. Chessboard pattern and fracture exposure order inside a subfield

4. K. Nakajima and N. Aizaki, "Calculation of a Proximity Resist Heating in Variably Shaped Electron Beam Lithography", *J. Vac. Sci. Technol. B* 10(6) (1992), pp. 2784-2788.
5. H. Sakurai, T. Abe, M. Itoh, A. Kumagae, H. Anze and I. Higashikawa, "Resist Heating Effect on 50keV EB Mask Writing", *SPIE Symposium on Photomask and X-Ray Mask Technology VI*, SPIE Vol. 3748, 1999, pp. 126-136.
6. Lee H. Veneklasen, "Optimizing Electron Beam Lithography Writing Strategy Subject to Electron, Optical, Pattern, and Resist Constraints", *J. Vac. Sci. Technol. B* 9(6) 1991, pp. 3063-3069.
7. S. Babin and I. Kuzmin, "Throughput optimization of electron beam lithography in photomask fabrication regarding acceptable accuracy of critical dimensions", *21st Annual BACUS Symposium on Photomask Technology*, Proc. SPIE, Vol. 4562, 2002, pp. 545-551. 16, 1998, 3241.
8. K. Kikuchi, H. Ohnuma and H. Kawahira, "New Optimization Method of the Exposure with Alternative Phase Shifting Masks", *Photomask and Next-Generation Lithography Mask Technology VIII*, SPIE Vol. 4409, 2001, pp. 41-51.
9. J.C. Lagarias, "Well-Spaced Labelings of Points in Rectangular Grids", *SIAM Journal of Discrete Math*, 13(4), 2000, pp 521-534.
10. Garey, M.R., and Johnson, D.S., *Computers and Intractability*. W.H. Freeman and Co., San Francisco (1979).

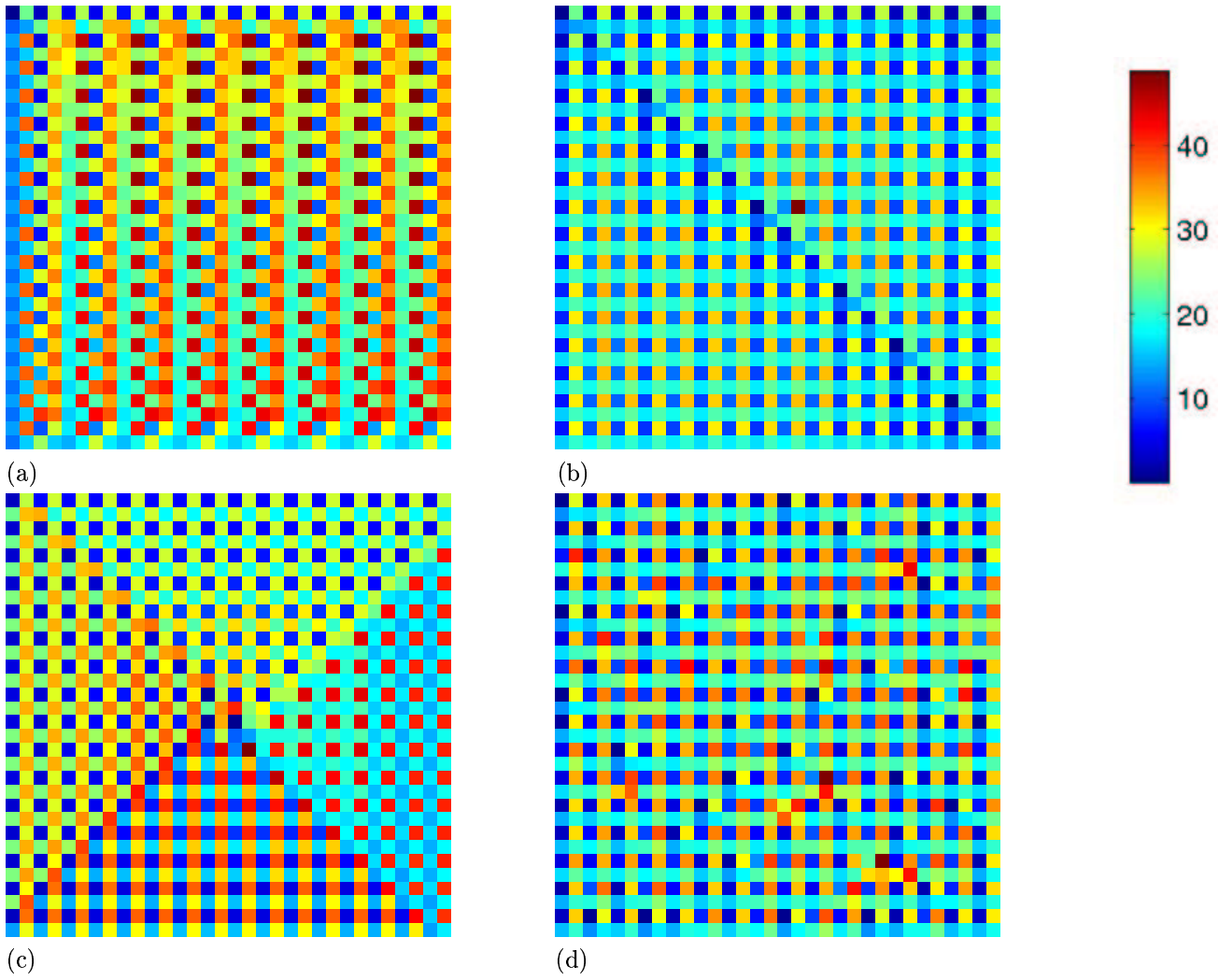


Figure 4. Thermal profile of 16×16 subfields for four writing schedules: (a) sequential, (b) Lagarias, (c) spiral, and (d) random. The color code shown is used for all writing schedules.

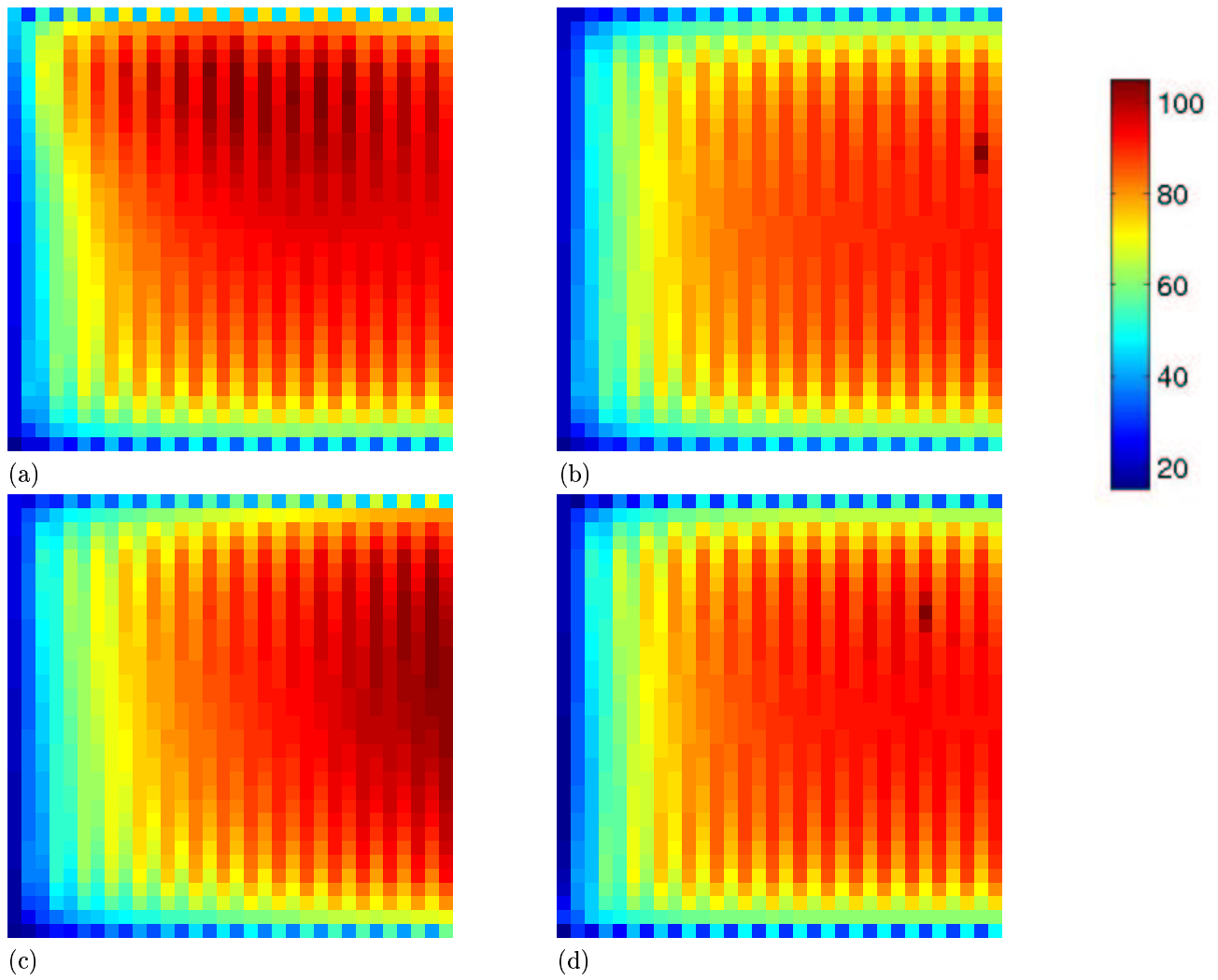


Figure 5. Thermal profile of the critical subfield (the subfield with maximum temperature) for four writing schedules: (a) sequential, (b) Lagarias, (c) spiral, and (d) random. The color code shown is used for all writing schedules.